ELSEVIER

Polymer 41 (2000) 6295–6299

polymer

Topographical modifications in PADC polymer under electron beam irradiation

C. Darraud-Taupiac[a,*], V. Binsangou[a], R. Isabey[b], E. Duverger[b], J.L. Decossas[a], L. Makovicka[b], J.C. Vareille[a]

[a]*IRCOM-C2M (Institut de Recherche en Communications Optiques et Microondes, Equipe Capteurs Microélectroniques et Microoptiques), Université de Limoges, 123, Av. A.Thomas, 87060 Limoges Cedex, France*

[b]*LMIT (Laboratoire de Métrologie des Interfaces Techniques), Université de Franche-Comté, BP 427, 25211 Montbeliard Cedex, France*

Received 29 September 1999; received in revised form 23 November 1999; accepted 24 November 1999

Abstract

A study of the topographical modifications of a PADC polymer substrate under 25 keV-Electron Beam (EB) irradiation is presented. The thickness variations as a function of the electronic fluence are systematically measured and show a fall in thickness. The causes of this phenomenon are discussed. Simulations of the interaction of the 25 keV-EB and the polymer are also carried out with the aim to correlate the deposited energy and the thickness variations.

Keywords: Polymer; Electron Beam; Thickness variations

1. Introduction

The interest in polymeric materials under irradiation and their applications to the field of optical telecommunication are well known. Numerous studies concerning polymers (PMMA, PMMI, BCB,…) under γ-rays or ion beam [1,2] have shown that they undergo chemical, physical and particularly optical modifications [3]. In the case of ion beam, it leads to a sufficient increase of the refractive index to allow the fabrication of optical waveguides [4–7]. We recently showed the feasibility of such optical structures in a PADC polymer under Electron Beam (EB) [8,9] and the work presented in this paper is part of a larger study on the application of the technique of EB irradiation to the field of integrated optics [10–12]. Pursuing this aim, the purpose here is the analysis of the topographical changes induced by the EB. An experimental study of the thickness variations as well as a theoretical simulation of the spatial energy distribution in the material are performed.

2. Experimental

2.1. Material—irradiation conditions—topographical variations analysis

Poly(diethylene glycol bis(allyl carbonate)) known as PADC or also CR-39 resin is a highly crosslinked network polymer with the repeat unit shown in Fig. 1. It is prepared by chain-growth polymerization involving both allyl groups and the polymerization is initiated by free radicals.

The samples used in this work were prepared by bulk polymerization of liquid monomer using diisopropyl peroxydicarbonate (IPP) as the initiator. The curing regime, as used by Ahmad and Stejny [13] (4 h at 45°C; 4h at 49°C; 4 h at 56°C; 2 h at 65°C; and 2 h at 85°C, in succession) was employed with the initiator concentration ranging from 1.5 to 10%. Previous work has shown [14] that the initiator concentration controls the conversion of the monomer and the density of crosslinks of the network, the latter reaching a maximum at the initiator concentration of about 5%.

In this study, the samples have been cured with an IPP concentration of 6% and present a glass transition temperature T_g of 90°C. The sample slabs have a parallel-piped shape of dimensions $15 \times 15 \times 1\ mm^3$. They are polished and coated with a 20 nm thick Au–Pd layer to avoid charge-up during EB exposure.

* Corresponding author. Tel.: +33-5-55-45-72-42; fax: +33-5-55-45-72-88.

E-mail address: darraud@unilim.fr (C. Darraud-Taupiac).

0032-3861/00/$ - see front matter
PII: S0032-3861(99)00862-9

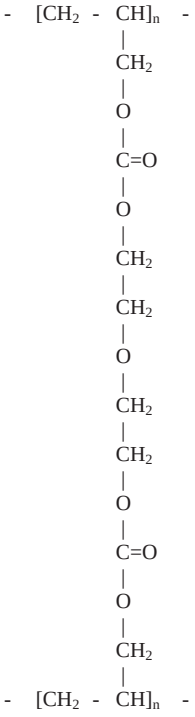

Fig. 1. PADC repeat unit.

The irradiations are performed using a Philips XL20 Scanning Electron Microscope (SEM) delivering accelerating voltages between 0.1 and 30 kV. The typical electronic energies used are 10–30 keV. Table 1 summarizes the irradiation conditions used in this work. The irradiation mode on an area has been chosen in view of the application of the work, which is the optical characterization of these preliminary obtained structures (refractive index measurements, determination of the index profiles,…).

The profile of the surface and hence the thickness variation measurement are realized with a SLOAN DEKTAK IIa profilometer (see Fig. 2) with a repeatability of about 0.2 μm.

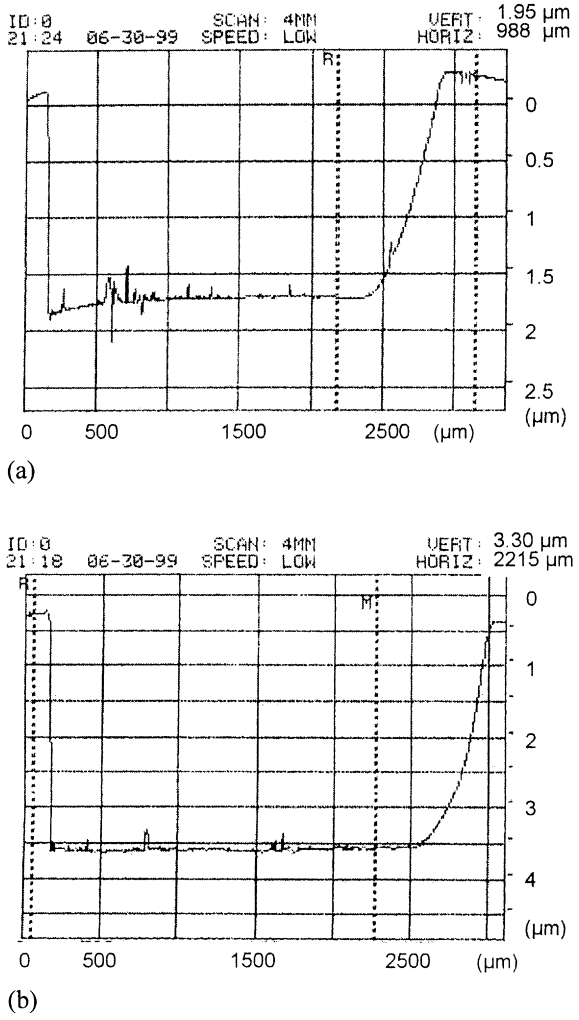

Fig. 2. A screen print of the profilometer showing surface variation with scan length for various fluences of a 25 keV-EB:(a) 8.8×10^{15} e/cm^2; (b) 3×10^{16} e/cm^2.

3. Results

3.1. Thickness variations Δe

The topographical modifications have been studied as a function of the electronic fluence Φ as it is shown in Fig. 3. An empiric law has been determined, similar to the one obtained by Nordman et al. [15] on amorphous AS_2S_3 films:

$$\Delta e = K(1 - \exp(-a\Phi))$$

The calculated values of the coefficients K and a are 3.4 μm and 1.05×10^{-16} cm^2/e, respectively. The thickness decrease reaches a few microns, which can be explained by a strong compaction or/and ablation process. This point will be discussed in Section 4.

We are also interested in the link between volume deposited energy density D_v of the EB into the substrate and Δe (Fig.4). The average D_v has been calculated in a superficial

Table 1
Summary of the irradiation conditions

EB-energy (keV)	Spot size (μm)	Irradiation mode	Dimensions (μm^2)	Probe current (nA)	Fluence Φ (e/cm^2)	Fluence rate $\dot{\Phi}$ (e/cm^2 s)
25	1	Area	2500×2500	40–70	3×10^{15}–8×10^{16}	2.2×10^{12}

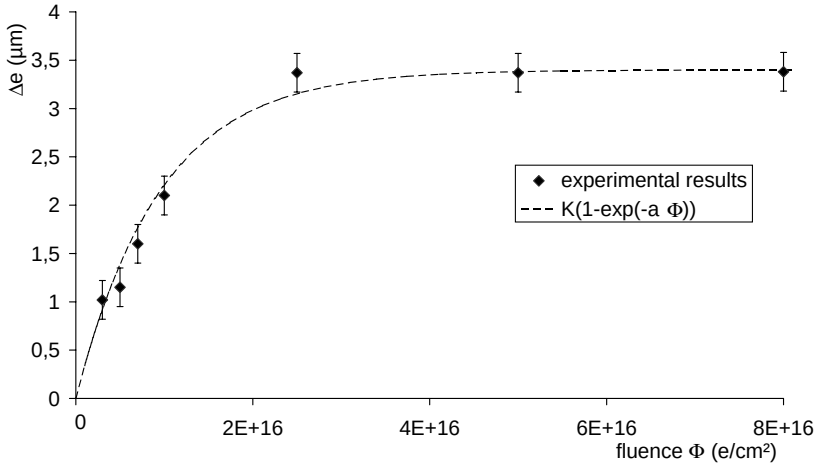

Fig. 3. Thickness variation as a function of the fluence of a 25 keV-EB $K = 3.4$ μm $a = 1.05 \times 10^{-16}$ cm^2.

substrate layer [6], arbitrarily chosen to have a thickness of $\lambda_0/4$, where λ_0 is the refractive index measurement wavelength, for a EB having an initial energy E_0, the density D_v is given by:

$$D_v(E_0) = \frac{4}{\lambda_0} \Phi \int_0^{\lambda_0/4} \left(\frac{dE}{dx}\right)_{E_0}(x)\, dx$$

where Φ is the fluence and $(dE/dx)_{E0}(x)$ is the linear stopping power at a depth x for an EB having an initial energy E_0.

This latter coefficient [16] corresponds to the contribution of the EB interaction with each of the components (C, H, O) of the polymer and results in the sum of the collision stopping power and the radiative stopping power. At the energy of 25 keV, the collision contribution is the predominant phenomenon.

From Figs. 3 and 4, it appears that the thickness variation shows an increase with increasing fluence or D_v and then a saturation.

3.2. Simulations: theoretical study of the energy distribution

The theoretical study is based on the EGS4-PRESTA code [17–19], to determine the distribution of the energy in 3D. The PADC substrate is characterized by its composition and density. The shape of the sample is parallel-piped and is constituted by $5 \times 5 \times 1$ μm^3 cells. In this work, each cell of the surface received a 25 keV-EB fluence of 4×10^6 e/cm^2. The width of the irradiated area has been set to 100 μm. The results of Figs. 5–7 give us some information about the distribution of the deposed energy in the material.

Figs. 5 and 6 present the isoenergy lines for a 25 keV-EB as a function of the fluence and the relative deposited energy versus the depth, respectively. They both show that the maximum of the EB-energy (around 95%) is lost in the seven firsts microns of the substrate. A 7-μm-deep cut

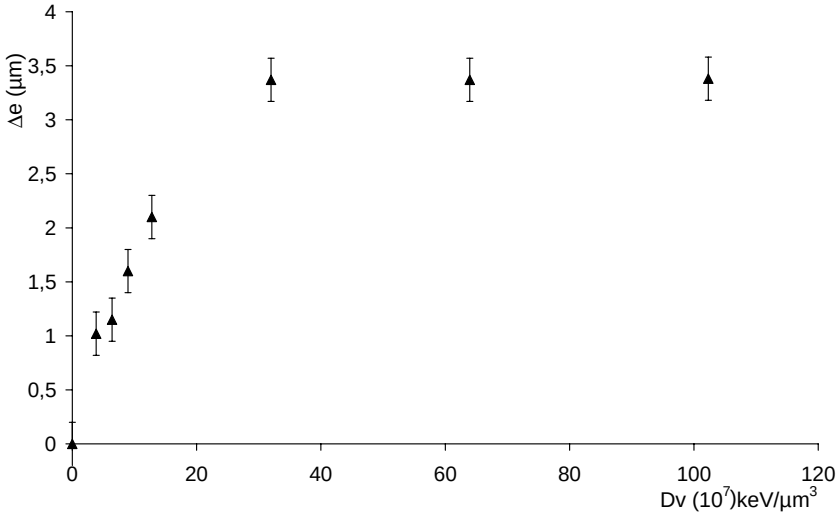

Fig. 4. Thickness variation as a function of the deposited energy of a 25 keV-EB.

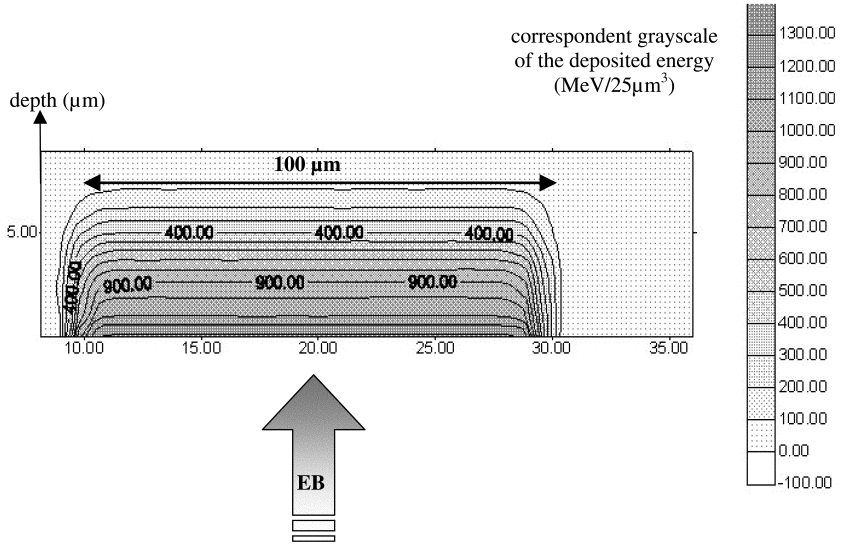

Fig. 5. Isoenergy lines for a 25 keV-EB (simulations data).

presented on Fig. 7 indicates that the broadening of the beam is negligible.

4. Discussion

The electrons flux induces various processes in the PADC polymer. Our interest here is focused on the thickness variation phenomenon. The material presents an amorphous and strongly heterogeneous structure, constituted by a single macromolecule. The deposition of energy generates an increase of the temperature on the irradiated zone, which makes the migration of chemical species toward the depth of the material easy and hence, causes a compaction of the medium. Profilometry measurements show a fall in thickness, which reaches saturation because the density cannot indefinitely increase. As the Au/Pd layer remains after irradiation and perfectly follows the profile of the irradiated area, without any damage, it can be assumed that the intimate structure of the polymer is still preserved.

The threshold effect of the compaction process is observable either on the profile measurements or on the relative deposited energy as a function of the depth curve. The calculated *K* coefficient of the Fig. 3 accounts for this effect.

5. Conclusion

This study showed that an EB irradiation of the PADC polymer induces a thickness variation of the material with a

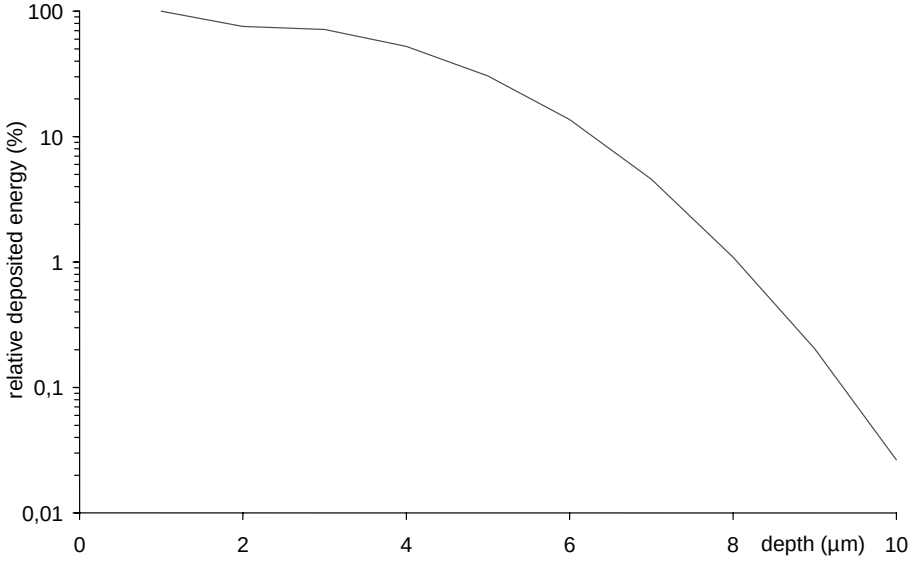

Fig. 6. Relative deposited energy as a function of depth for a 25 keV-EB (simulations data).

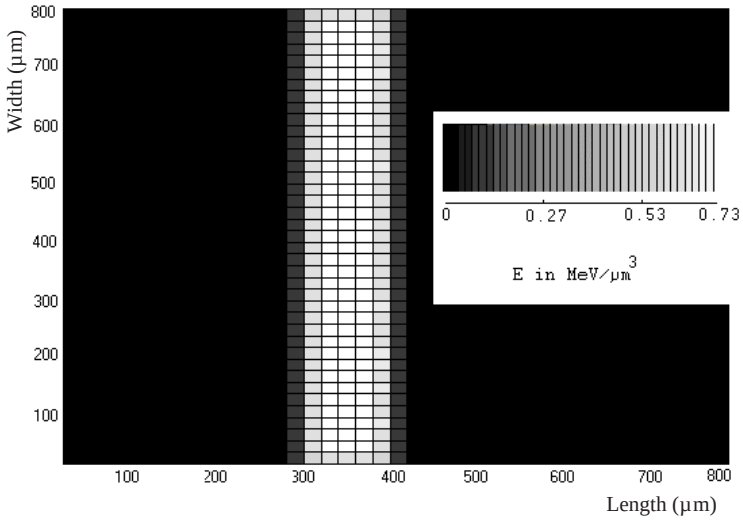

Fig. 7. Density of energy deposited in PADC under 25 keV-EB at a depth of 7 μm, sample size: $800 \times 800 \times 40$ μm^3, fluence: 3×10^{16} e/cm^2 (simulations data).

Δe maximum value of about 3.4 ± 0.2 μm. This process has been attributed to a compaction of the material related with the energy deposition of the electrons in the substrate, obtained thanks to the achieved simulations.

In parallel to this work, a complete study of the relation between the refractive index variation obtained using the EB technique and the energy deposition gradient is in progress. Moreover the low dispersion of spatial repartition of the energy should allow the definition of accurate 3D optical structures and therefore enable this technique to be used in the field of Optoelectronics.

Acknowledgements

We wish to thank Professor J. Stejny (H.H. Wills Physics Laboratory, Bristol University, UK) for fabricating the samples.

References

[1] Chapiro A. Radiat Phys Chem 1960;14:101.
[2] Charlesby A. In: Dupuy C, editor. Applied sciences, 8. 1975.
[3] Mazzoldi P, Arnold GW, editors. Ion beam modifications of insulators. Amsterdam: Elsevier, 1987. p. 302. chap. 8.
[4] Bennamane B, Decossas JL, Marcou J, Vareille JC. Micro-Optics 1988;1014:132–5.
[5] Kulish JR, Franke H, Singh A, Lessard RA, Knystautas EJ. Appl Phys 1988;63:2517.
[6] Bennamane B, Decossas JL, Gagnadre C, Vareille JC. Nucl Instrum Methods 1991;B62:103–8.
[7] Rück DM, Schulz J, Deusch N. Nucl Instrum Methods 1997;B131:149–58.
[8] Binsangou V, Darraud-Taupiac C, Decossas JL, Vareille JC. Journées Nationales d'Optique Guidée. Nice, October, proceedings. JNOG96, No. 36, 1996.
[9] Darraud-Taupiac C, Binsangou V, Decossas JL, Vareille J.C. Proceedings of the European-Materials Research Society (EMRS) 1999 Spring Meeting, 1–4 Juin 1999, Strasbourg, France. Symposium Materials, Technologies and Applications for Optical Interconnect, paper K-I-8.
[10] Fujino T, Maeda H, Kimura Y, Horibe H, Imanaga Y, Shinkawata H, Nakao S, Kato T, Matsui Y, Hirayama M, Yasuoka A. Jpn J Appl Phys 1996;35:6320–7.
[11] Cumming DRS, Thoms S, Beaumont SP, Weaver JMR. Appl Phys Lett 1996;68(3):322–4.
[12] Erikson N, Hagberg M, Larsson A. Vac Sci Technol B 1996;14(1):184–6.
[13] Portwood T, Stejny J. Nucl Tracks Radiat Meas 1984;8:151–4.
[14] Ahmad S, Stejny J. Nucl Tracks Radiat Meas 1991;19:11.
[15] Nordman N, Salminen O, Kuittinen M, Turunen J. Appl Phys 1996;80(7):3683–6.
[16] Stopping Powers for electrons and positrons. International Commission on Radiation units and Measurements (ICRU), report 37, 1 October 1984.
[17] Nelson WR, Hirayama H, Rogers DWO. The EGS4 Code System. Stanford Linear Accelarator Center Report SLAC-265 (Stanford, CA 94305) 1985.
[18] Bielajew AF, Rogers DWO. PRESTA: the parameter reduced electron-step transport algorithm for electron Monte-Carlo transport. Nucl Instrum Methods 1987;B18:165–81.
[19] Duverger E, Isabey R, Huguet M, Makovicka L. Quelques remarques pratiques pour les utilisateurs de EGS4 sous DOS 6.2. Radioprotection 1997;32(2):229–35.